

Lateral tunneling and ballistic transport in two-dimensional electron gas devices defined by nanostructure gates

C. P. Umbach, A. Palevski, M. Heiblum, and U. Sivan

IBM Research Division, Thomas J. Watson Research Center, Yorktown Heights, New York 10598

(Received 31 May 1989; accepted 7 July 1989).

Novel, laterally configured, tunneling hot electron transfer amplifier (THETA) devices have been formed using nanostructure metal gates to induce potential barriers separating emitter, base, and collector regions in a two-dimensional electron gas. The gates were formed by a liftoff technique using PMMA resist and a high resolution electron beam writing tool. Lateral electron tunneling has been directly observed, using electron energy spectroscopy, through potential barriers under metal gates as wide as 52 nm. The energy distribution of the hot electrons was only ≈ 5 meV wide. Certain gate configurations were found to increase the fraction of emitted electrons which reached the collector. Current gain as high as 105 was observed. This is better than the best results previously obtained with vertical THETA devices.

I. INTRODUCTION

Advances in lithographic capabilities have frequently led to faster devices due to a reduction in the transit time of carriers, and the smaller RC time constants, in miniaturized devices. The ability to reduce device dimensions can also lead to the creation of devices based on phenomena operative only on a relatively smaller size scale. One example of such a device is the tunneling hot electron transfer amplifier (THETA) device.¹ The ballistic motion of electrons in a THETA device results in an enhanced operating speed relative to conventional, larger transistor devices in which the effective carrier velocity is limited by diffusive scattering. Promising results have been obtained with THETA devices fabricated using molecular beam epitaxy to layer precisely defined emitter, base, collector, and barrier regions in GaAs/AlGaAs heterostructures.^{2,3,4} This "vertical" device configuration, however, has a number of drawbacks due to fabrication problems resulting, in part, from difficulties in making Ohmic contacts to the thin base region, and from a short scattering length in the heavily doped base which limits gain. A number of recent studies⁵ have shown that metal gates can be used to define conducting channels in the two-dimensional-electron-gas (2DEG) that can be produced in GaAs/AlGaAs heterostructures. High mobility heterostructures with relatively long elastic scattering lengths ($\lambda \geq 1 \mu\text{m}$) have now become fairly common. Since gain in THETA devices is enhanced by long elastic scattering lengths, an attempt was made to create isolated emitter, base, and collector regions in a 2DEG by lithographically patterning narrow gates on GaAs/AlGaAs heterostructure surfaces. The potential barriers under the gates proved⁶ to be thin enough to permit appreciable tunneling, and the performance of the resulting "lateral" THETA devices has turned out to be even better than the best results obtained with vertical structures. This paper will discuss the fabrication and characterization of lateral THETA devices, emphasizing processing details that proved to play a significant role in determining the device performance.

II. EXPERIMENTAL

The GaAs/AlGaAs heterostructures were formed using molecular beam epitaxy. On top of an undoped GaAs layer, an undoped AlGaAs "spacer" layer (AlAs mole fraction 34%) ranging between 8 and 40 nm thick was grown. The AlGaAs deposition was then interrupted and a sheet of Si atoms, with an areal density of $\approx 3 \times 10^{12} \text{ cm}^{-2}$, was deposited under an overpressure of As ("planar doping"). The Si atoms supplied electrons to the 2DEG. The Si was followed by 20 nm of undoped AlGaAs, and a 5–15 nm thick GaAs "cap" layer. Typically the 2DEG carrier density at $T = 4.2 \text{ K}$ was $3 \times 10^{11} \text{ cm}^{-2}$ and the mobility was $3 \times 10^5 \text{ cm}^2/\text{V s}$.

After the heterostructure was patterned with photoresist, the exposed surface was etched using a mixture of 1 part phosphoric acid, 1 part hydrogen peroxide, and 50 parts water, in order to destroy the 2DEG everywhere except the protected "mesa" region. After stripping the resist mask, conventional AuGeNi contact pads and registration marks were formed by patterning additional photoresist and lifting off a sequentially evaporated multilayer metal film. The metal film consisted of 5 nm Ni, followed by 20 nm Ge, 40 nm Au, 10 nm Ni, and 100 nm Au. Annealing at $T = 420\text{--}450 \text{ }^\circ\text{C}$ for 30 s under an Ar/H_2 atmosphere created Ohmic contacts to the 2DEG wherever the pads overlapped the edge of the mesa. Pads which did not overlap the mesa, and therefore did not contact the 2DEG, were used to contact the metal gates formed later on top of the mesa.

Metal gates were patterned on top of the heterostructure using electron beam nanolithography and a high resolution scanning transmission electron microscope (STEM) under IBM PC-AT computer control. Flexible computer software permitted triangles, trapezoids, rectangles, and angled lines to be written in resist. The high resolution (1 nm beam diameter) obtained in the STEM is at the cost of a maximum writing field of only $\approx 130 \mu\text{m}$ and a focused, relatively undistorted, field size of only $\approx 50 \mu\text{m}$. To get around this limitation, computer controlled stepping motors attached to micrometers were used to position samples. Angular align-

ment of the samples was accomplished manually using tweezers and a low power optical microscope. A double layer of resist consisting of ≈ 20 nm 2041 PMMA (MW 360 000) on ≈ 60 nm 2010 PMMA (MW 150 000) was used for the electron beam exposures. Proximity corrections to the exposure were made by trial and error. Exposed PMMA was developed for 60 s in a 1:2 mixture of methyl isobutyl ketone and isopropyl alcohol. Evaporation of 20 nm of AuPd, followed by liftoff in acetone, resulted in gated GaAs/AlGaAs heterostructures. An example of the final structure is shown in Fig. 1.

The device pads were bonded using both thermal compression of Au wire and ultrasonic bonding of Al wire. Measurements were performed using a Hewlett-Packard #4145B Semiconductor Parameter Analyzer in a common base configuration.

III. RESULTS AND DISCUSSION

The one-dimensional potential energy of a lateral THETA device is shown in Fig. 2. The device consists of an emitter (E), base (B), and collector (C) region separated by potential barriers. The potential barrier between emitter and base is produced by a negative bias (V_{EB}) on the emitter gate, while the potential barrier between base and collector is produced by negative bias (V_{BC}) on the collector gate. In contrast to a vertical THETA device^{2,3,4}, the heights of the potential barriers in a lateral THETA device can be continuously and independently adjusted. With suitable voltages applied to the gates, biasing the emitter negative with respect to the base (V_{EB}) results in a current from the emitter (I_E). The emitter current is divided between a base current (I_B) and a collector current (I_C). The barrier (Φ_C) between base and collector can be lowered either by decreasing the collector gate voltage or biasing the collector positive with respect to the base (V_{CB}). With the biases illustrated in Fig. 2, emitted electrons will arrive and be thermalized in the collector

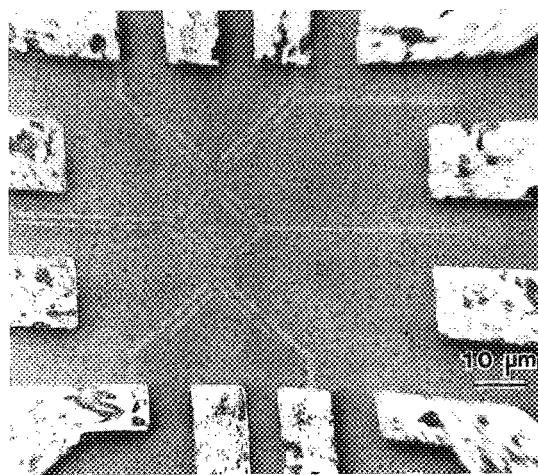


FIG. 1. Electron micrograph showing AuPd gates patterned on top of a mesa chemically etched out of a GaAs/AlGaAs heterostructure. AuGeNi pads thermally diffused into the edges of the mesa contact the 2DEG. The AuPd gates overlapped AuGeNi pads which did not touch the mesa. A negative bias on the gates formed potential barriers in the 2DEG in the mesa.

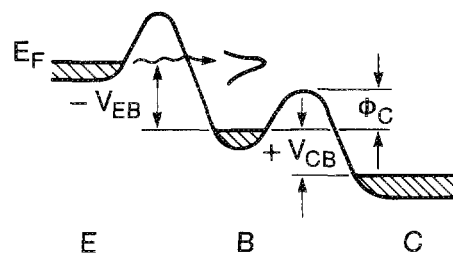


FIG. 2. 1D potential energy vs distance for a lateral THETA device. In vertical THETA devices the potential barriers are thinner but of fixed height. The potential barriers in lateral devices can be tuned by varying the bias on the gates.

unless they are first scattered in the base so that they no longer have sufficient energy to surmount the collector barrier. A measure of device quality is given by the transfer ratio, $\alpha = I_C/I_E$. Current gain β is given by $I_C/I_B = \alpha/(1 - \alpha)$.

A lateral THETA device consisting of AuPd gates on top of a GaAs/AlGaAs heterostructure is shown in Fig. 3(a). Devices were made with a variety of gate widths > 35 nm, and a separation between gates ranging from 50 nm to several microns. Wide gate regions away from the device induced long potential barriers which blocked parallel conduction in the mesa around the device. The flared gate pattern permitted electrical contact to the base. Contacts to the 2DEG on both sides of the base were used to directly monitor the base resistance.

Since the continuity of the gates can be determined by their ability to deplete the 2DEG underneath them, electrical contact was typically made to only one end of the gate. In spite of the absence of an apparent current path through the nanostructure gates, numerous precautions were still necessary to prevent static discharges from destroying the gates. In addition, it was observed that samples became extremely sensitive to electrical breakdown between the contact pads if the pads were patterned ≈ 2 μm apart. This problem no longer occurred when the pad separation was increased to 10 μm .

Reasonable current gain in a THETA device can be achieved only if electrons are emitted directionally towards the collector via tunneling and not in random directions by thermal emission. In vertical THETA devices^{3,4}, the high, potential barrier produced by the band discontinuity at GaAs/AlGaAs interfaces ensured that all emission was by tunneling. In lateral THETA devices with much wider gates, however, tunneling through an induced potential barrier had to be demonstrated. This was accomplished using a form of electron energy spectroscopy in which the top of the collector barrier was used to determine the energy distribution of the emitted electrons reaching the collector. Figure 3(b) shows the variation of I_C with the spectrometer voltage, V_{CB} for a device similar to that in Fig. 3(a), but with gates 52 nm wide. The "knee" structure in the curve around $V_{CB} = -10$ meV is characteristic of electron tunneling in a THETA device. The collected current is given by $I_C = A \int_{\Phi_C}^{\infty} e n(E) v(E) dE$, where A is the area, $n(E)$ is the energy distribution of the electrons arriving at the spectrom-

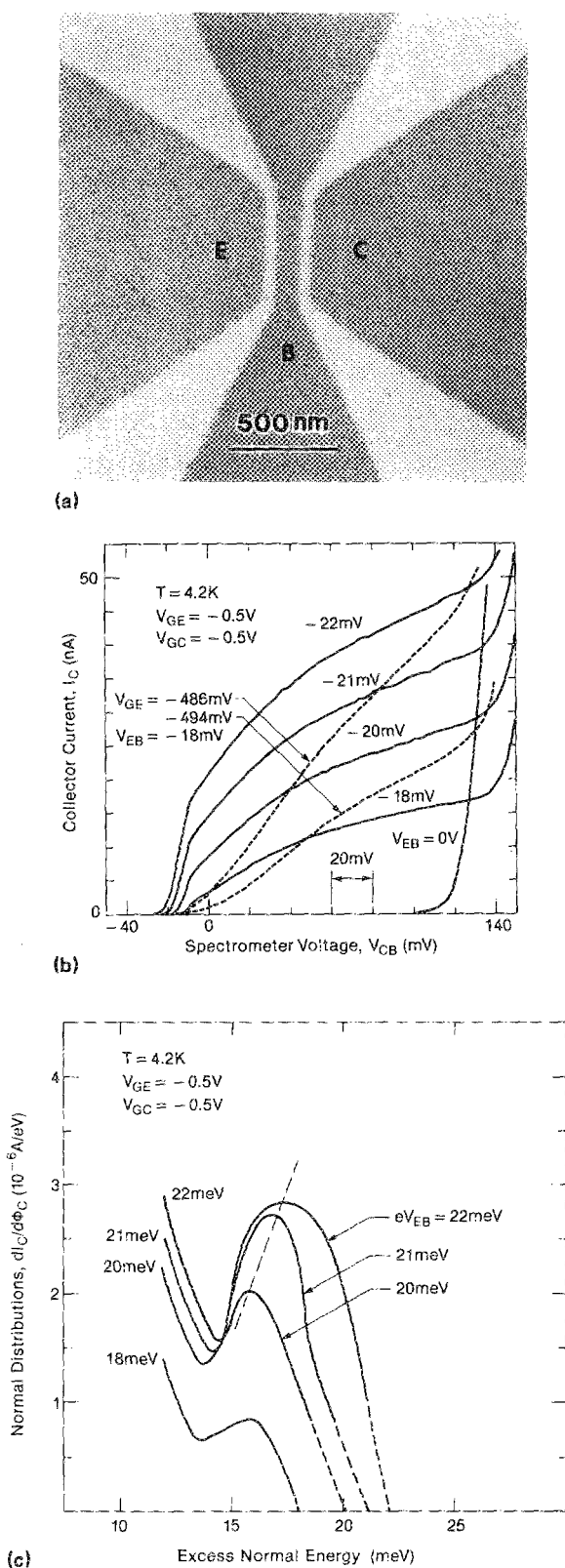


FIG. 3. (a) Electron micrograph of a lateral THETA device formed by patterning AuPd gates on top of a GaAs/AlGaAs heterostructure. Biasing the gates negative with respect to the 2DEG results in the formation of emitter, base, and collector regions separated by adjustable potential barriers. Ohmic contacts are made to the 2DEG in each of the regions. (b) Collector current vs spectrometer voltage for a lateral THETA device. The "knee" around $V_{CB} = -10\text{ mV}$ is a characteristic sign of electron tunneling. (c) Normal energy distribution for hot electrons relative to the Fermi energy in the base. The peak in the distribution $\sim 4\text{ meV}$ below the Fermi energy in the emitter is a clear demonstration of tunneling.

eter, and E and v are the energy and velocity associated with the electrons traversing normal to the gate. Over a small energy range $v(E)$ is fairly constant and $n(E) \approx dI_C/d\Phi_C = (dI_C/dV_{CB})/(d\Phi_C/dV_{CB})$, for a constant injection energy V_{EB} . (dI_C/dV_{CB}) can be determined directly from the device characteristics. $(d\Phi_C/dV_{CB})$ can be determined by setting V_{CB} to various values and equating Φ_C with the value of V_{EB} at which I_C increases rapidly from zero. Figure 3(c) shows the normal energy distribution of electron surmounting the collector barrier. The peak in the distribution approximately 4 meV below the Fermi energy in the emitter is clear evidence of tunneling. The relatively narrow width of the energy distribution, $\approx 5\text{ meV}$, reflects the wider potential barriers and the lower Fermi energy usually occurring in the lateral devices.

No clear evidence of size quantization in the base, or resonant tunneling, was observed in lateral THETA devices with electrically continuous bases. It was found that the base conductance in devices with relatively thin spacer layers could be easily pinched off by biasing the emitter and collector gates. In addition, the base exhibited conductance fluctuations as it was pinched by biasing the emitter and collector gates. These fluctuations occurred with greater frequency as the spacer thickness was decreased. A crude analysis of the device structure suggests that this effect may be due to random fluctuations in the spacing of Si atoms in the planar doping layer. These positional fluctuations may be reflected in potential fluctuations on the order of the Fermi energy in base regions where the low electron concentration results in very poor electrostatic screening. Random defects inherently present even in high mobility GaAs may also play a role in producing the fluctuations. Both the unintentional pinching off of the conductance, and the potential fluctuations, in the base were minimized through the use of thicker spacer layers.

The ballistic transfer ratio α_B for the results in Fig. 3 is ≈ 0.25 at $V_{CB} = 0$. It was found that α could be increased by adjusting the gate patterns in a number of ways. Simply increasing the ratio of the collector to emitter gate lengths by a factor of 3 increased α_B to about 0.7 for a device with a base width d_B of $\approx 170\text{ nm}$, by collecting "stray" electrons coming from the corners of the emitter. Assuming $\alpha_B \approx \exp(-d_B/\lambda)$ leads to an elastic scattering length $\lambda = 480\text{ nm}$. This lower limit on λ suggests that the elastic scattering length for hot electrons is of the same order as that for cold electrons. Another means of increasing α was implemented by patterning gates inside the emitter region, as shown in Fig. 4(a). Increasing the voltage on these gates inside the emitter served to block the access of electrons to the sides of the emitter. When combined with a collector gate designed to capture all electrons emitted nonorthogonal to the emitter, α increased to above 0.99, as shown in Fig. 4(b). Figure 4(c) shows that the current gain for this device reached $\beta = 105$. These results were obtained with the collector barrier low enough to just isolate the collector from the base. Although some fraction of the collected electrons have been scattered in the base, this high value for β is better than the best results previously obtained with vertical THETA devices⁴ ($\beta = 41$). Leakage over the potential barriers, probably due

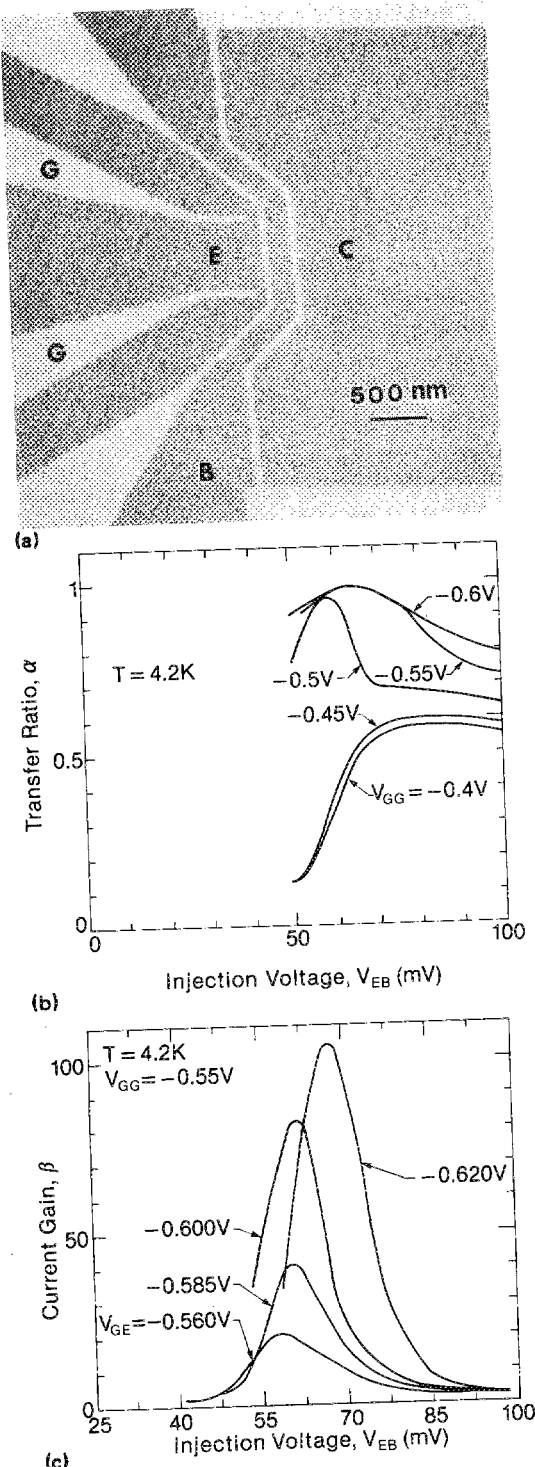


FIG. 4. (a) Electron micrograph of a lateral THETA device configuration. (b) Transfer ratio vs injection voltage designed to enhance the device gain. (c) Current gain for various voltages on the gates (G,G) inside the emitter. (c) Current gain vs injection voltage. The drop in β above 72 meV is due to the emission of a phonon.

to random potential fluctuations, made it impossible to do spectroscopy at lower V_{EB} 's to determine the energy distribution in this device. A decrease in current gain above $V_{EB} \approx 72$ meV results from the emission of a longitudinal optical phonon.^{7,8}

IV. SUMMARY

Electron tunneling through the potential barrier induced by metal gates in a 2DEG has been established through the use of electron energy spectroscopy. Lateral THETA devices have been formed by patterning nanostructure gates in a variety of configurations. The maximum current gain ($\beta \approx 105$) is higher than the best previous results obtained with vertical THETA devices. Hot, ballistic electrons with narrow energy distributions (≈ 5 meV), and elastic scattering lengths comparable to those of cold electrons, have been observed. Random potential fluctuations appear to exert a marked influence on the behavior of these small devices.

ACKNOWLEDGMENTS

The authors are grateful to A. N. Broers and R. Koch for assistance with the electron beam lithography; C. M. Knoedler, L. Osterling, H. Shtrikman, and M. Weckwerth for help with sample processing; P. Solomon and F. Stern for helpful discussions. The work was supported in part by the U. S. Defense Advanced Research Projects Agency and administered by ONR Contract No. N00014-87-C-0709.

- ¹M. Heiblum, Solid State Electron. **24**, 343 (1981).
- ²J. R. Hayes, A. F. J. Levi, and W. Wiegmann, Phys. Rev. Lett. **54**, 1570 (1985).
- ³M. Heiblum, M. I. Nathan, D. C. Thomas, and C. M. Knoedler, Phys. Rev. Lett. **55**, 2200 (1985).
- ⁴K. Seo, M. Heiblum, C. M. Knoedler, J. E. Oh, J. Pamulapati, and P. Bhattacharya, IEEE Electron. Device Lett. **10**, 73 (1989).
- ⁵B. J. van Wees, H. van Houten, C. W. J. Beenakker, J. G. Williamson, L. P. Kouwenhoven, D. van der Marel, and C. T. Foxon, Phys. Rev. Lett. **60**, 848 (1988); D. A. Wharam, T. J. Thornton, R. Newbury, M. Pepper, H. Ahmed, J. E. F. Frost, D. G. Hasko, D. C. Peacock, D. A. Ritchie, and G. A. C. Jones, J. Phys. C **21**, L209 (1988).
- ⁶A. Palevski, M. Heiblum, C. P. Umbach, C. M. Knoedler, A. N. Broers, and R. H. Koch, Phys. Rev. Lett. **62**, 1776 (1989).
- ⁷A. Palevski, C. P. Umbach, and M. Heiblum, Appl. Phys. Lett. **55**, 1421 (1989).
- ⁸U. Sivan, M. Heiblum, and C. P. Umbach, Phys. Rev. Lett. **63**, 992 (1989).